Research Article

Synthesis and Characterization Of (E)-4-Chloro-2-((4-(Dimethylamino)-2-Hydroxybenzylidene) Amino) Phenol and (E)-4-Bromo-N-(Pyridin-2-Ylmethylene) Aniline Towards Biological Evaluation of Antimicrobial, Antioxidant, Molecular Docking, and ADMET Studies

Kalpana Rajendran [1*], Divya Dhakshinamurthy [2], Shemalavathi Ezhumalai[3], Vinay Kumar[4]

[1]Institute of Biotechnology, Department of Bioengineering, Saveetha School of Engineering, Saveetha Institute of Medical and Technical Sciences (SIMATS), Thandalam, Chennai 602 105, Tamil Nadu, India.
[2]Department of Chemistry, Vel Tech Rangarajan Dr. Sagunthala R&D Institute of Science and Technology, Avadi, Chennai, Tamil Nadu, India.
[3]K S Raja Arts And Science College for Women, Gingee, Villupuram, Tamil Nadu, India 604210.
[4]Biomaterials and Tissue Engineering Laboratory (BITE LAB), Department of Community Medicine, Saveetha Medical College and Hospital, Saveetha Institute of Medical and Technical Sciences (SIMATS), Chennai, Thandalam 602105, India.

Corresponding author: Kalpana Rajendran

Abstract

Halogenated Schiff a versatile class of biologically active compounds with potential antimicrobial and antioxidant properties. In this present study, two novel derivatives, (E)-4-chloro-2-((4-(dimethylamino)-2-hydroxybenzylidene)amino)phenol (CDHBP) and (E)-4-bromo-N-(pyridin-2-ylmethylene)aniline (BPMA), were synthesized via condensation reactions and it's physico-chemical characterization was done by ^{1}H NMR, and ^{13}C NMR spectroscopy. Their biological activities, such as antimicrobial, Minimum Inhibitory Concentration (MIC), antioxidant, and hemolytic compatibility was done. CDHBP showed antifungal activity against Candida albicans (MIC = 32 µg/mL) but showed moderate antibacterial effect, while BPMA shows moderate antibacterial activity for Staphylococcus aureus and Enterococcus faecalis. Hemolytic studies confirmed the biocompatibility of CDHBP at 500 ug/mL as 6% of lytic properties. Molecular docking analysis showed excellent interactions (binding energy -7.60 and strong hydrogen bond interaction) of CDHBP with lanosterol 14-demethylase and in silico ADMET analysis shows high intestinal absorption with low cardiotoxic and hepatotoxic risks, however it's low solubility and potential genotoxicity requires further investigation. Overall, the study focus on importance of structural relevance on the biological and pharmacokinetic profiles of halogenated Schiff bases and provides a understating of its therapeutic potential for future optimization toward drug development.

Keywords: Schiff bases, Antimicrobial, Biocompatibility, Molecular docking, ADMET.

Introduction

Schiff bases, formed by the condensation of primary amines with carbonyl groups of compound, with different pharmacological activities, such as anticancer, antiviral, anti-inflammatory and antimalarial properties(1). The wide spectrum of biological efficacy is often results to the imine (-C=N-) linkage, which play important role formation with metal ions and interaction with multiple biological targets(2). The addition of halogen atoms into Schiff base structures can enhance biological potency and specificity by modifying electronic and steric properties(3). Therefore, this structural modification often leads to improved lipophilicity and bioavailability, which are important factors for drug efficacy(4). This study focus on synthesis, characterization, and biological evaluation of novel halogenated Schiff base derivatives, aiming to elucidate the structure-activity relationships which are important for developing new therapeutic agents with antimicrobial and antioxidant properties antimicrobial, antioxidant, and toxicological profiles to identify promising candidates for therapeutic development(5). The presence of intramolecular hydrogen bonds between the hydroxyl group of the phenolic ring and azomethine nitrogen often enhance their stability, while the inclusion of electron-withdrawing halogen groups on the aromatic ring can significantly amplify their antifungal and antibacterial activities(6). Particularly, thiazole and imidazopyridine based Schiff base derivatives have demonstrated excellent antibacterial and antifungal properties, gives a rich area for further screening in halogenated analogues(7). The unique structural features of Schiff bases, particularly the imine bond and the potential for metal chelation, provide a versatile platform for designing compounds with targeted biological activities(8).

Invasive fungal infections lead to serious threat to public health, specifically those receiving chemotherapeutic treatment, organ transplant recipients, and patients diagnosed with HIV/AIDS(9). Among most common and dangerous infections are those caused by Candida sp. which showed increased patient morbidity and mortality worldwide(10). The severity of these infections is aggregate by alarming rise of antifungal drug resistance to current antifungal agents(11). Fungi have developed by various mechanisms to escape its antifungal agents, including changes in drug targets, increased drug efflux, and formation of biofilms, rendering current therapeutic as less effective(12). This urgent and escalating crisis demands continue to discover and develop novel antifungal agents with novel mechanisms to prevail resistance and improve patient outcomes(13). Among these, Schiff

bases and pyridine derivatives have emerged as particularly promising classes of compounds due to their flexible synthesis and broad spectrum of biological activities(4). The exploration of such novel structures gives a pathway to identifying novel compounds capable of targeting fungal pathogens through different pathways. Here, we report the synthesis of novel halogenated Schiff bases (E)-4-chloro-2-((4-(dimethylamino)-2-hydroxybenzylidene)amino)phenol and (E)-4-bromo-N-(pyridin-2-ylmethylene)aniline, characterized by FT-IR, ^{1}H NMR, and ^{13}C NMR. We evaluated their antimicrobial activity, hemolytic safety, antioxidant potential, and ADMET properties, with docking rationalizing CDHBP's moderate activity against C. albicans. These findings develop structure-activity understandings for fungal pathogens.

Materials and methods

Typical procedure for the synthesis of (E)-4-chloro-2-((4-(dimethylamino)-2-hydroxy benzylidene)amino)phenol (CDHBP)

A mixture of 2-amino-4-chlorophenol and 2-hydroxybenzaldehyde in EtOH stirred at 25 °C for 4 hrs (Scheme 1). The thin layer chromatography was used during the reaction process to observe using the process. After reaction completion, the crude product was separated by aqueous solvent separation (ethyl acetate and water) the extraction was done twice and the solvent was condensed under reduced pressure. The combined organic extracts were dried over anhydrous Na_2SO_4, filtered, and concentrated. For the purification silica gel column chromatography were used until separation of pure compound. Yield if possible, MASS and FTIR ^{1}H NMR (400 MHz, $CDCl_3$) δ = 8.40 (s, 2H), 7.20 (d, J=8.8, 3H), 7.07 (d, J=2.3, 5H), 6.91 (d, J=9.3, 3H), 6.29 (dd, J=8.9, 2.5, 3H), 6.19 (d, J=2.4, 3H), 3.42 (q, J=7.1, 14H), 2.17 (s, 13H). ^{13}C NMR (101 MHz, $CDCl_3$) δ 166.15, 153.87, 151.58, 148.90, 132.51, 130.05, 128.09, 123.84, 122.99, 108.06, 104.61, 98.01, 44.38.

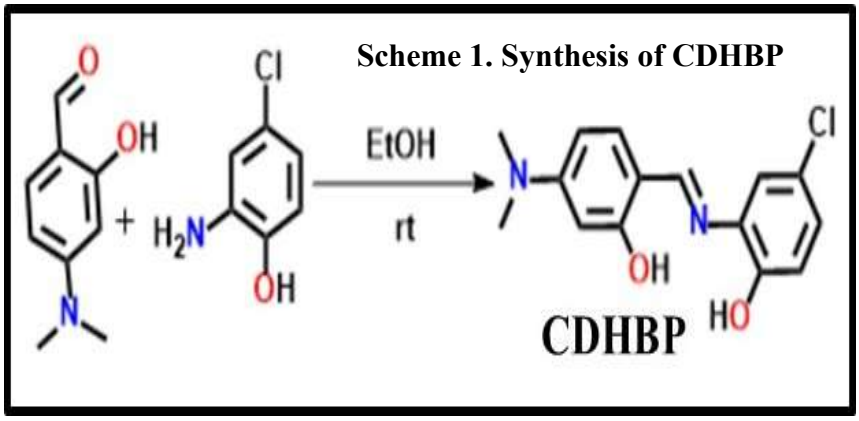

Typical procedure for the synthesis of (E)-4-bromo-N-(pyridin-2-ylmethylene)aniline (BPMA)

A mixture of 4-bromoaniline and picolinaldehyde in ethanol was mixed at ambient temperature for 4 hours (Scheme 2). Thin-layer chromatography was used during the reaction to monitor its progress. After reaction completion, the crude product was separated by an aqueous solvent system (ethyl acetate and water). The extraction was done twice, and the solvent was condensed under reduced pressure. The combined organic extracts were dried over anhydrous Na_2SO_4, filtered, concentrated under reduced pressure, and purified by column chromatography to give BPMA. Yield if possible, MASS and FTIR ^{1}H NMR (400 MHz, $CDCl_3$) δ = 8.72 (ddd, J=4.8, 1.7, 0.9, 1H), 8.59 – 8.56 (m, 1H), 8.18 (dt, J=7.9, 1.0, 1H), 7.82 (d, J=1.6, 1H), 7.55 – 7.52 (m, 2H), 7.39 (ddd, J=7.5, 4.8, 1.2, 1H), 7.18 – 7.15 (m, 2H). ^{13}C NMR (101 MHz, $CDCl_3$) δ 193.43, 161.63, 161.05, 154.28, 149.92, 149.79, 137.07, 136.74, 132.32, 132.00, 127.86, 125.35, 122.79, 122.02, 121.72, 120.25, 116.69, 29.70

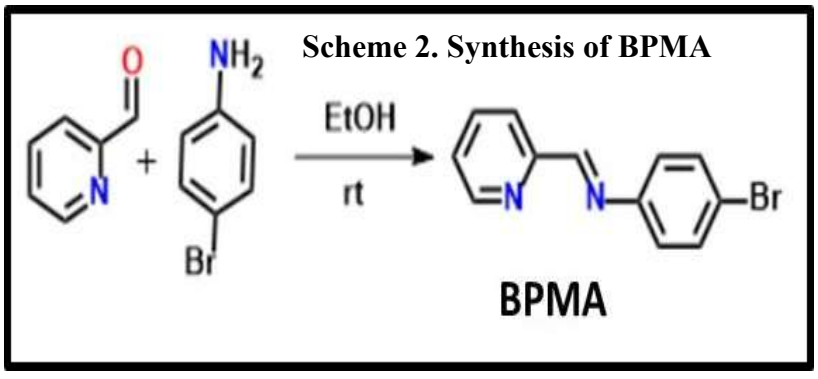

Antimicrobial activity by well diffusion assay of CDHBP and BPMA

The antimicrobial activities of synthesized molecules CDHBP and BPMA were initially screened using the agar well diffusion assay against selected bacterial and fungal pathogens. Overnight cultures of these pathogens were prepared to an optical density (OD_{600}) of 0.4 in sterile Mueller-Hinton Broth (MHB). Using sterile cotton swabs, the standardized microbial culture evenly lawned on the surface of Mueller-Hinton Agar (MHA) plates. The wells were made by punching into the agar using a sterile cork borer. Aliquots of prepared CDHBP and BPMA at concentrations were loaded into the respective wells, followed by overnight incubation of plates at 37 °C. The growth inhibition was measured as diameters of the zones of inhibition using a zone scale, and the results were recorded for analysis.

Minimum Inhibitory Concentration of CDHBP and BPMA

The minimum inhibitory concentrations (MIC) of the test compounds CDHBP, BPMA, and commercially available antibiotics were determined employing 96-well microtiter plates. The MIC assay was carried out according to the guidelines of the Clinical and Laboratory Standards Institute (CLSI) and the European Committee on Antimicrobial Susceptibility Testing (UCAST). Test pathogens were grown in MHB. Serial dilutions of CDHBP and BPMA were dispensed into 96-well plates, followed by the addition of 5 µL of overnight-grown human pathogens per well. The plates were incubated at 37°C for 16 hrs. Following incubation, 100 µL of (5 mg/mL) MTT dye was introduced into all wells and kept in the dark for 30 min. Dimethyl sulfoxide was subsequently added as a solubilizing agent and permitted to stand for 15–30 min. Inhibition of growth was measured by assessing optical density at 595 nm using an ELISA plate reader.

Antioxidant activity of CDHBP and BPMA

The DPPH radical scavenging activity was employed to determine the antioxidant capacity of CDHBP and BPMA. Different concentrations of CDHBP and BPMA was prepared in 96 well plates, followed by the addition of 100 µL of a freshly prepared 0.2 mM DPPH solution. Samples were incubated in dark conditions for 30 mins, after which absorbance was recorded at 517 nm using a spectrophotometer. The percentage of DPPH radical scavenging activity, serving as a measure of compound's antioxidant potential, was computed via the equation: % DPPH scavenging = [(Ablank - Asample) / Ablank] x 100, where Ablank represents the absorbance of the DPPH solution without CDHBP and BPMA and absorbance of the reaction mixture containing CDHBP and BPMA.

Hemolytic activity of CDHBP

The hemocompatibility of CDHBP with human red blood cells (RBC) was assessed. The RBCs obtained from volunteers were washed twice with phosphate-buffered saline. Various concentrations of CDHBP were prepared in PBS, 100 µL RBCs were added, and the mixture was incubated for 30 mins at 37 °C. Absorbance at 570 nm was measured to quantify hemoglobin release. PBS served as the negative control and 1% Triton X-100 as the positive control. The hemolysis percentage was calculated from these measurements.Hemolysis Percentage = (A_{540} of test compounds) – (A_{540} of PBS)/[(A_{540} of 1% Triton x-100)-(A_{540} of PBS)]×100

Molecular docking analysis

Protein and Ligand Preparation

The crystal structure of lanosterol 14α-demethylase (PDB ID: 5EQB) from Saccharomyces cerevisiae, complexed with itraconazole and featuring an intact transmembrane domain, was retrieved from the Protein Data Bank. Preparation of the 5EQB structure involved removal of water molecules and addition of charges via PyMOL. The ligand CDHBP was designed using ChemDraw Ultra, exported as a PDB file, and next energy-minimized in Avogadro employing the universal force field with the steepest descent method.

Docking Procedure

Docking of the refined 5EQB receptor against the CDHBP ligand was performed using AutoDock 4.2 software. Kollman partial charges and polar hydrogens were added to the receptor, followed by conversion to PDBQT format. The ligand underwent addition of hydrogens and designation of torsional degrees of freedom prior to PDBQT conversion. A grid box the active site was defined with dimensions of 60 × 40 × 40 Å and a grid spacing of 0.375 Å. Simulations utilized the Lamarckian genetic algorithm with standard parameters, executing 100 runs. Outcomes were assessed by hydrogen bonding profiles, binding affinities, root-mean-square deviation values, and predicted inhibitory concentrations (IC_{50}), prioritizing the highest-populated binding clusters.

ADMET Profiling

Physicochemical properties, along with absorption, distribution, metabolism, excretion, and toxicity parameters of CDHBP, were predicted via the ADMETlab 2.0 webserver69. Compliance with Lipinski's Rule of Five for drug-likeness was evaluated on the

pkCSM platform. The compound was first transformed into SMILES notation using ChemDraw Ultra and then submitted to pkCSM for analysis.

Results

The formation of pure CDHBP and BPMA is identified by their ^{1}H and ^{13}C NMR spectra recorded in $CDCl_3$ solvent, and TMS is an internal standard. The ^{1}H NMR spectrum of CDHBP shows the presence of appropriate protons in the aromatic and aliphatic region (Figure 1).

Figure 1. ^{1}H NMR spectra of CDHBP in $CDCl_3$

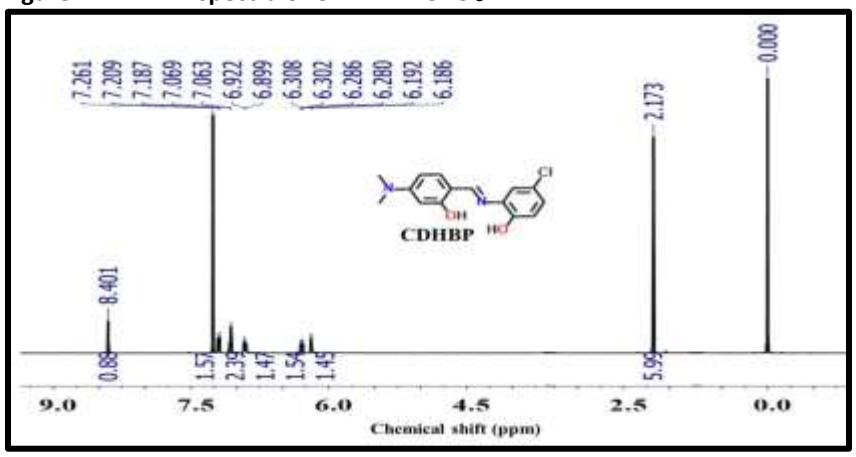

The formation of the imine linkage is confirmed by sharp singlet at δ 8.40 ppm, which is assigned to azomethine proton (-CH = N-)(14). The presence of six aromatic proton peak suggests the formation of CDHBP. Additionally, a high-intensity six-proton singlet at δ 2.17 ppm confirm the presence of two methyl groups of the N,N -dimethylamino substituent. Absence of other peaks from 0 to 9 ppm suggests that CDHBP has no impurities. The ^{13}C NMR spectrum (recorded in $CDCl_3$) further confirms the carbon framework of CDHBP, displaying the expected signals, including both aromatic and aliphatic carbons (Figure 2). In the aliphatic region, the highly intense signal at δ 44.38 ppm is linked to two equivalent methyl carbons of the -dimethylamino substituent.

Figure 2. ^{13}C NMR spectra of CDHBP in $CDCl_3$

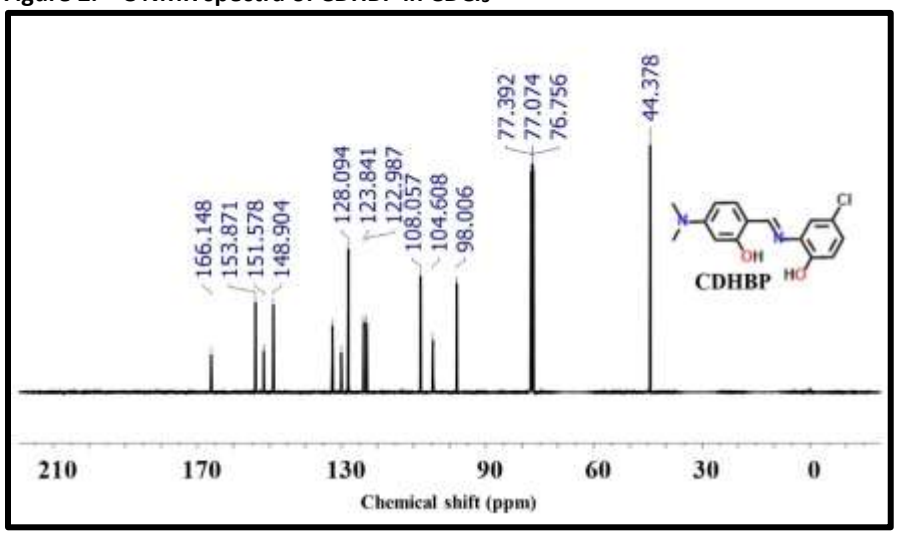

On the other hand, The ^{1}H NMR spectrum of the synthesized Schiff base, BPMA confirms its structural framework as the expected proton is present (Figure 3).

Figure 3. ^{1}H NMR spectra of BPMA in $CDCl_3$

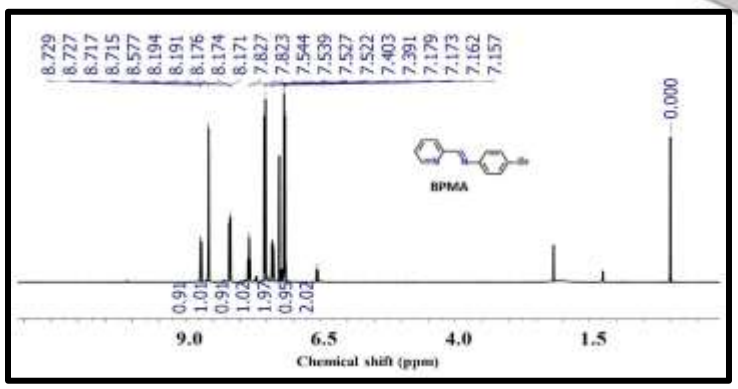

All the eight-aromatic protons appeared clearly between δ 8.729 ppm to δ 7.157 ppm. The ^{13}C NMR spectrum of **BPMA** confirms the presence of all the aromatic carbon atoms (**Figure 4**). Absence of other noticeable peaks in Figure 3 and 4 suggests the formation of BPMA with high purity.

Figure 4. ^{13}C NMR spectra of BPMA in $CDCl_3$

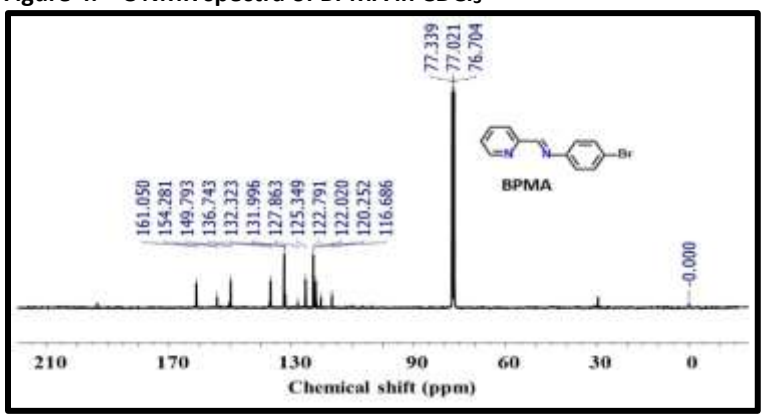

Antimicrobial activity of CDHBP and BPMA

The antimicrobial activity of the synthesized CDHBP and BPMA, was evaluated against a different of clinical pathogens including Gram-positive bacteria (S. aureus, E. faecalis), Gram-negative bacteria (E. coli, P. aeruginosa), and the fungal pathogen C. albicans by well diffusion assay. The BPMA shows moderate Zone of Inhibition (ZOI) for 12mm against S. aureus and 13 mm for E. faecalis and P. aeruginosa there is no ZOI for E. coli and C. albicans, whereas CDHBP shows high zone of inhibition for C. albicans (15 mm) and moderate ZOI for S. aureus and E. faecalis (12 mm) and no ZOI for E. coli and P. aeruginosa (Fig.5 and Table. 1).

Fig. 5. Antimicrobial activity BPMA and CDHBP

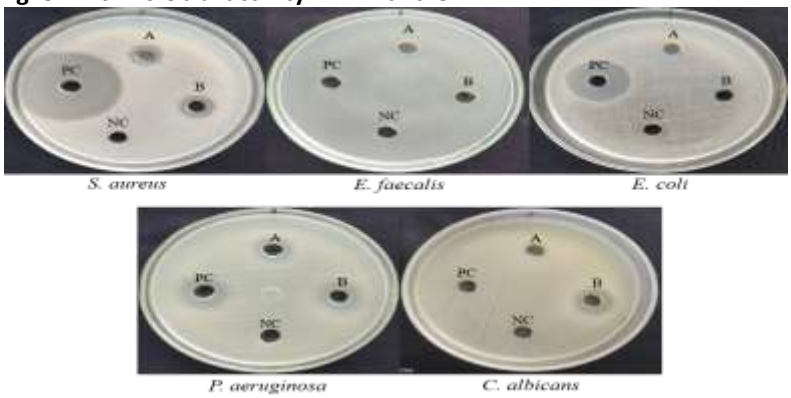

A: 1 mg/mL; B: 2 mg/mL; C: 5 mg/mL; NC: Negative control

Table1. Antimicrobial activity of synthesized molecule against clinical pathogens

Compound	Zone of Inhibition in mm				
	Gram-positive bacterium		Gram-negative bacterium		Fungal pathogen
	S. aureus	E. faecalis	E. coli	P. aeruginosa	C. albicans
BPMA	12	13	-	13	-
CDHBP	12	12	-	-	15
NC	-	-	-	-	-
PC	34	18	24	16	-

Minimum Inhibitory Concentration (MIC) of CDHBP and BPMA

The MIC of CDHBP and BPMA were determined against selected pathogens. The BPMA exhibited an MIC at 256 µg/mL against S. aureus and E. faecalis and there is no growth inhibition for E. coli, P. aeruginosa and C. albicans. For CDHBP, the MIC value was found at 32 µg/mL against C. albicans followed by 512 µg/mL for S. aureus and E. faecalis and no growth inhibition for E. coli and P. aeruginosa (Table. 2)

Antioxidant activity of CDHBP and BPMA

The antioxidant activity of CDHBP and BPMA was evaluated at concentrations. The BPMA showed moderate activity and concentration dependent activity, at 1000 µg/mL shows 51%, 500 µg/mL shows 19.5 %, and 250 µg/mL shows 6.5 % concentration, antioxidant activity for CDHBP was observed 6% at µg/mL, there is no activity was found below 500 µg/mL concertation (Figure. 6)

Figure. 6. Antioxidant activity of CDHBP and BPMA

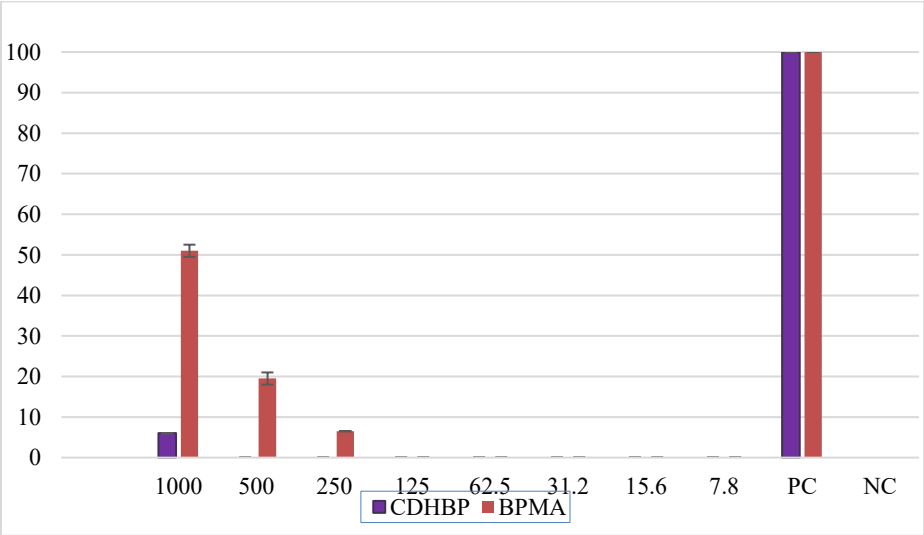

Hemolytic activity

The hemolytic activity of CDHBP at various concentrations. At a concentration of 1000 µg/mL, the hemolytic activity was 24%, this activity decreased with decreasing concentration, 6 % at 500 µg/mL, and 250 µg/mL showed 1.5% of lytic activity. For all other concentrations below 250, no hemolytic activity was observed (Fig. 7).

Table.2. MIC of CDHBP and BPMA in mm

Figure. 7. Hemolytic activity of CDHBP

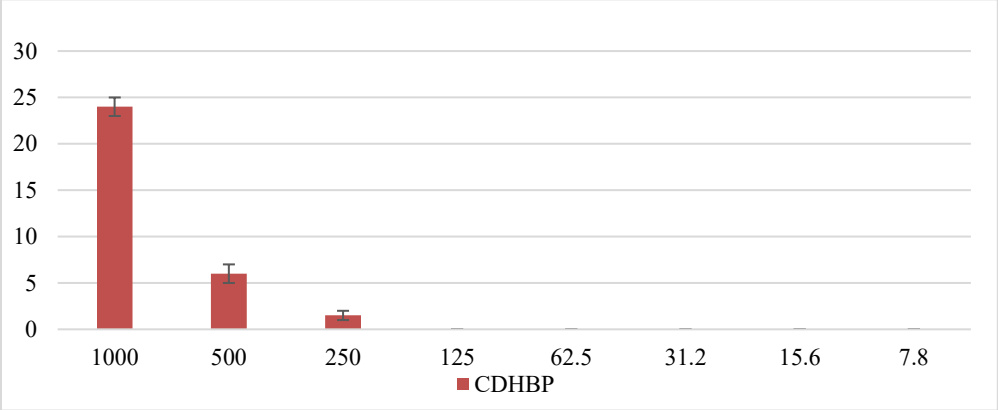

Molecular docking

Molecular docking analysis was performed to predict the binding interactions of CDHBP with the lanosterol 14- α demethylase protein (PDB ID: 5EQB) from Saccharomyces cerevisiae. The simulations found two significant binding poses. Pose 1 exhibited the most favorable binding energy of -7.56 kcal/mol and a ligand efficiency of -0.38. Its inhibition constant was calculated to 2.86 µM. This optimal pose was stabilized by several key hydrogen bond interactions, specifically between A:ARG385:HH11 and an oxygen atom on the ligand, between a hydrogen atom of TYR126 and an oxygen atom on the ligand, between a hydrogen atom on the ligand and an oxygen atom of A:SER382, and between the HN of A:SER382 and an oxygen atom on the ligand. Other energy components for Pose 1, such as intermolecular energy (-9.05 kcal/mol), van der Waals, hydrogen bond, and desolvation energy (-8.87 kcal/mol). In comparison, Pose 2 displayed slightly less favorable binding, with a binding energy of -7.1 kcal/mol, a ligand efficiency of -0.36, and a higher inhibition constant of 6.27 µM (Fig. 8).

Figure. 8. Molecular docking analysis of CDHBP with lanosterol 14- α demethylase protein

Pose - 1

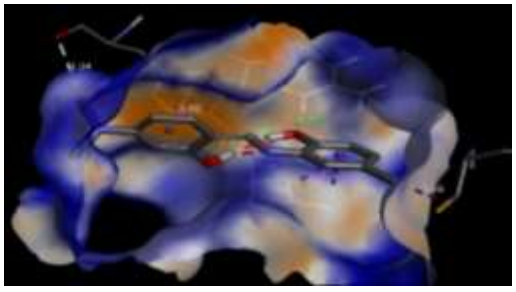

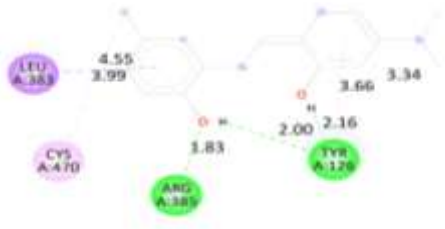

Pose - 2

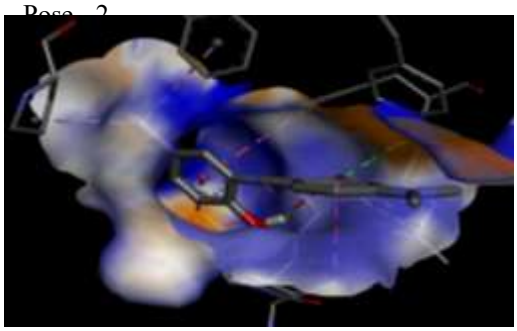

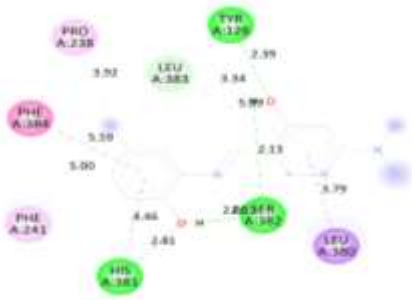

Table. 3. Docking properties of CDHBP against 14- α demethylase protein for pose 1 and pose 2

S. no	Property	Pose 1 Value	Pose 2 Value
1	Binding energy	-7.56	-7.1

2	Ligand efficieny	-0.38	-0.36
3	Inhibition constant	2.86	6.27
4	Intermol energy	-9.05	-8.59
5	Vdw_hb_desolv_energy	-8.87	-8.45
6	Electrostatic energy	-0.19	-0.14
7	Total_internal	-1.88	-1.81
8	Torsinal_energy	1.49	1.49
9	Unbound energy	-1.88	1.89
10	Hydrogen bond interaction	A:ARG385:HH11 – 1:O 1:H_TYR126:OH	1:H – A:SER382:O A:SER382:HN – 1: 1:O

ADMET analysis

The physicochemical and ADMET properties of CDHBP were computationally predicted. CDHBP has a molecular weight of 290.75, a LogP of 3.5678, 3 rotatable bonds, 4 acceptors, 2 donors, and a surface area of 122.13. For absorption, the molecule demonstrates high human intestinal absorption (91.469%) and Caco2 permeability (1.364 log Papp in 10^{-6} cm/s) but exhibits low water solubility (-4.601 log mol/L) and poor skin permeability (-2.873 log Kp). It is also predicted to be a P-glycoprotein substrate, though not an inhibitor of P-glycoprotein I or II. In terms of distribution, CDHBP shows moderate blood-brain barrier permeability (0.071 log BB) but low central nervous system permeability (-1.909 log PS), with a human steady-state volume of distribution of -0.339 log L/kg and a fraction unbound of 0.158. Metabolic predictions indicate that CDHBP is not a substrate for CYP2D6 or CYP3A4, nor is it an inhibitor of CYP2C9, CYP2D6, or CYP3A4; however, it is predicted to inhibit CYP1A2 and CYP2C19. Excretion is characterized by a total clearance of 0.175 log ml/min/kg, and it is not a renal OCT2 substrate. Toxicity assessment suggests AMES toxicity and a maximum tolerated dose in humans of 1.362 log mg/kg/day. Reassuringly, CDHBP is not predicted to be hepatotoxic, skin sensitizing, or an inhibitor of hERG I or hERG II. Further ecotoxicity data include a T. Pyriformis toxicity of 2.208 log ug/L and minnow toxicity of 0.659 log mM (Table.4).

Table 4. ADMET properties of CDHBP

Category	Property	Value	Unit
Molecule	Molecular Weight	290.75	
Molecule	LogP	3.5678	
Molecule	#Rotatable Bonds	3	
Molecule	#Acceptors	4	
Molecule	#Donors	2	
Molecule	Surface Area	122.13	
Absorption	Water solubility	-4.601	log mol/L
Absorption	Caco2 permeability	1.364	log Papp (10^-6 cm/s)
Absorption	Intestinal absorption	91.469	%
Absorption	Skin permeability	-2.873	log Kp
Absorption	P-gp substrate	Yes	
Absorption	P-gp I inhibitor	No	
Absorption	P-gp II inhibitor	No	
Distribution	VDss	-0.339	log L/kg
Distribution	Fraction unbound	0.158	Fu
Distribution	BBB permeability	0.071	log BB
Distribution	CNS permeability	-1.909	log PS
Metabolism	CYP2D6 substrate	No	
Metabolism	CYP3A4 substrate	No	
Metabolism	CYP1A2 inhibitor	Yes	

Metabolism	CYP2C19 inhibitor	Yes	
Metabolism	CYP2C9 inhibitor	No	
Metabolism	CYP2D6 inhibitor	No	
Metabolism	CYP3A4 inhibitor	No	
Excretion	Total clearance	0.175	log ml/min/kg
Excretion	Renal OCT2 substrate	No	
Toxicity	AMES toxicity	Yes	
Toxicity	Max tolerated dose	1.362	log mg/kg/day
Toxicity	hERG I inhibitor	No	
Toxicity	hERG II inhibitor	No	
Toxicity	Oral rat acute toxicity (LD50)	2.61	mol/kg
Toxicity	Oral rat chronic toxicity (LOAEL)	1.751	log mg/kg/day
Toxicity	Hepatotoxicity	No	
Toxicity	Skin sensitisation	No	
Toxicity	T. Pyriformis toxicity	2.208	log ug/L
Toxicity	Minnow toxicity	0.659	log mM

Discussion

The synthesized halogenated Schiff base derivatives, CDHBP and BPMA, showed structure-dependent antimicrobial and antioxidant activities, consistent with the role of the azomethine group in enhancing efficacy(15). The HOMO–LUMO energy gap and dipole moment correlated with membrane permeability, drug excretion, and biological properties(16). Drug-likeness and pharmacokinetic profiles, including oral absorption and plasma protein binding, supported their potential(17). Chlorinated chalcone studies showed halogen position effects on electron distribution and antimicrobial activity(18). Spectroscopic characterization and quantum studies confirmed structures linked to activities(19). Chelation in metal complexes increased lipophilicity and bacteriostatic action compared to ligands(20). The CDHBP showed moderate antibacterial activity and antifungal activity against C. albicans (MIC 32 µg/mL), with favorable docking with lanosterol 14-α-demethylase (binding energy -7.56 kcal/mol, K_i 2.86 µM). A difference between docking and MIC was observed, as reported for other Schiff bases(21). Hydrazone derivatives showed bioactivity(22). Bioavailability limitations impacted value even with docking(23), with ADMET properties critical for target accumulation(24). Molecules lacking hydrogen bonds with lanosterol 14-α-demethylase exhibited activity via different pathways(25). Imidazole derivatives targeted Lanosterol 14 alpha-demethylase(26). Hydrogen bonding with residues like Cys470 or Arg489 supported CYP51 inhibition(27), and diisooctyl phthalate enhanced CYP51 binding efficiency(28). Physicochemical optimization may improve uptake and ADMET for CDHBP(29). The BPMA displayed moderate antibacterial activity for S. aureus and E. faecalis and P. aeruginosa and antioxidant activity (51 at 1000 µg/mL to 6.5 at 250 µg/mL). Triazole-bis-pyrazoles showed similar antifungal and antioxidant effects against C. albicans and C. neoformans(30). Lipophilicity improved antimicrobial efficiency(31), atomic arrangement influenced binding(32), and dual-action compounds targeted resistant pathogens(33). Molecular dynamics refined binding stability(34), with ADMET optimization and biofilm inhibition potential (35). The CDHBP hemolytic activity was low (24% at 1000 µg/mL, 0% below 250 µg/mL), shows as biocompatibility (35). ADMET showed high intestinal absorption, moderate BBB permeability, low hepatotoxicity/cardiotoxicity, but AMES positivity and CYP1A2/2C19 inhibition(29). Structural modifications increase the toxicity risks(36). Halogenation influenced outcomes variably; CDHBP showed selective antifungal activity, antioxidant potential, and safety, warranting further study, while CDHBP informed structure activity relationships.

Conclusion

This study successfully synthesized and evaluated two halogenated Schiff bases, CDHBP and BPMA. While CDHBP showed moderate antifungal activity against C. albicans (MIC 32 µg/mL) and promising binding interactions with lanosterol 14-α-demethylase, its efficacy was limited by low aqueous solubility and predicted AMES toxicity. The ADMET analysis of CDHBP showed high intestinal absorption and low cardiotoxic risk, though the difference between docking predictions and in vitro results highlights the influence of pharmacokinetic factors. Overall, these findings reveal that structural variations in Schiff bases

significantly modulate biological performance, providing a clear path for the future optimization of these compounds as potential therapeutic agents.

Acknowledgments
Not applicable.
Consent for Participate
Not applicable.
Consent to Publication
Not applicable.
Ethics Approval
This study does not involve experiments on animals or human subjects.
Informed Consent
Not applicable.
Declaration of Conflicting Interests
The authors declared no potential conflicts of interest with respect to the research, authorship, and/or publication of this article.
Funding
Not applicable.
Footnotes
Use of Artificial Intelligence-assisted Technology: During manuscript preparation, the authors used Grammarly Premium to correct language errors. This AI-assisted tool checked spelling, grammar, punctuation, clarity, and plagiarism, suggesting corrections were needed. This manuscript's quality by combining human expertise with AI efficiency.

References

1. Todarwal MA, Sancheti RS, Shah HH, Patil AM, Patil R, Bendre RS. Synthesis, Crystal structure, in vitro, and in silico biological studies of 2, 5-dihydroxybenzaldehyde based novel Schiff bases. Research Square (Research Square). 2023.
2. Obradović R, Joksimović N, Janković N, Kosanić M, Matić J, Milović E, et al. Discovery of Schiff bases as potent antibacterial and antifungal agents. New Journal of Chemistry. 2023;48(40):17492-9.
3. Rahman MZ, Islam MD, Haque MA, Rahman MM, Hossain ME, Sutradhar RK. Synthesis, Characterization, Molecular Docking Studies and Biological Evaluation of Thiazole Schiff Base Analogs. Asian Journal of Chemistry. 2024;36(3):649-54.
4. Oladipo SD, Adeleke AA, Badeji AA, Babalola KI, Labulo AH, Hassan I, et al. Computational investigation and biological activity of selected Schiff bases. Journal of the Nigerian Society of Physical Sciences. 2024:2103-.
5. H. Al-Tel T, A. Al-Qawasmeh R, F. Zaarour R. Design, synthesis and in vitro antimicrobial evaluation of novel Imidazo[1,2-a]pyridine and imidazo[2,1-b][1,3]benzothiazole motifs. European journal of medicinal chemistry. 2011;46(5):1874-81.
6. Waziri I, Masena HM, Yusuf TL, Coetzee LCC, Adeyinka AS, Muller A. Synthesis, characterization, biological evaluation, DFT and molecular docking studies of (Z)-2-((2-bromo-4-chlorophenyl)imino)methyl)-4-chlorophenol and its Co(ii), Ni(ii), Cu(ii), and Zn(ii) complexes. New Journal of Chemistry. 2022;47(38):17853-70.
7. Lemilemu F, Alem MB, Demissie TB, Eswaramoorthy R, Endale M. Synthesis, antibacterial and antioxidant activities of Thiazole-based Schiff base derivatives: a combined experimental and computational study. BMC Chemistry. 2021;15(1).
8. Liu Y, Hu LT, Liu B, Qu Z. Membrane-targeting antibacterial isoniazid schiff base against S. aureus and biofilms. Frontiers in Chemistry. 2025;13.
9. Sharma M, Chakrabarti A. Candidiasis and Other Emerging Yeasts. Springer Science+Business Media; 2023. p. 15-24.
10. Katsipoulaki M, Stappers MHT, Malavia D, Brunke S, Hube B, Gow NAR. Candida albicans and Candida glabrata : global priority pathogens. Microbiology and Molecular Biology Reviews. 2024;88(2).
11. Lee Y, Robbins N, Cowen LE. Molecular mechanisms governing antifungal drug resistance. 2023. p. 5-.
12. Fisher MC, Alastruey-Izquierdo A, Berman J, Bicanic T, Bignell E, Bowyer P, et al. Tackling the emerging threat of antifungal resistance to human health. Nature Portfolio; 2022. p. 557-71.
13. Liu D, Zhou R, Gao X. Recent innovations and challenges in the treatment of fungal infections. Frontiers Media; 2025. p. 1676009-.
14. Abedin MM, Pal TK, Uddin MN, Alim MA, Sheikh MC, Paul S. Synthesis, quantum chemical calculations, in silico and in vitro bioactivity of a sulfonamide-Schiff base derivative. Heliyon. 2024;10(14).
15. Cholan SS, Rajan AT, Kamalesu S, Subramanian R, Karuppaiah S, M AZ. Unveiling the Promising Pharmaceutical benefits of Newly Synthesized Schiff Base: DFT, Molecular docking, In silico ADME/T and PASS analysis. Research Square (Research Square). 2024.

16. Mannaa AH, Gomaa EA, Zaky R, Ghaith EA, El-Hady MNA. Bivalent transition metal complexes of triazole pyridine Schiff base with theoretical and biological investigations. Scientific Reports. 2025;15(1).
17. Pirzada AS, Khan H, Alam W, Darwish HW, Elhenawy AA, Kuznetsov AE, Daglia M. Physicochemical properties, pharmacokinetic studies, DFT approach, and antioxidant activity of nitro and chloro indolinone derivatives. Frontiers in Chemistry. 2024;12.
18. Ashburn BO. Computational Analysis of a Series of Chlorinated Chalcone Derivatives. Computational Chemistry. 2018;7(4):106-20.
19. Sindhu I, Singh A, Deswal Y, Kirar JS. Exploring Schiff base ligand and their transition metal complexes: synthesis, characterization, antimicrobial, ADME and computational insight as cholesterol lowering agents and anticancer activity on HeLa cells. Research on Chemical Intermediates. 2024;51(2):839-73.
20. Abdel-Rahman LH, Abdelghani AA, AlObaid AA, El-ezz DA, Warad I, Shehata MR, Abdalla EM. Novel Bromo and methoxy substituted Schiff base complexes of Mn(II), Fe(III), and Cr(III) for anticancer, antimicrobial, docking, and ADMET studies. Scientific Reports. 2023;13(1).
21. Emami L, Jamshidzadeh A, Khabnadideh S, Pakshir K, Jamshidi M, Rahat S, et al. In Vivo Antifungal Activity and Computational Studies of Some Azole Derivatives against Candida Albicans. Journal of chemistry. 2023;2023:1-12.
22. Ibraheem HH, Queen BK, Al-Sabti MD, Issa AA, Al-Majedy YK, Jabir MS, et al. Insights into the pharmaceutical properties and in silico study of novel hydrazone derivatives. Scientific Reports. 2024;14(1):29912-.
23. Okolo EN, Ugwu DI, Ezema BE, Ndefo JC, Eze FU, Ezema CG, et al. New chalcone derivatives as potential antimicrobial and antioxidant agent. Scientific Reports. 2021;11(1).
24. Kaur H, Singh J, Narasimhan B. Antimicrobial, antioxidant and cytotoxic evaluation of diazenyl chalcones along with insights to mechanism of interaction by molecular docking studies. BMC Chemistry. 2019;13(1).
25. Jadhav AK, KHAN PK, Karuppayil SM. PHYTOCHEMICALS AS POTENTIAL INHIBITORS OF LANOSTEROL 14 A-DEMETHYLASE (CYP51) ENZYME: AN IN SILICO STUDY ON SIXTY MOLECULES. International Journal of Applied Pharmaceutics. 2020:18-30.
26. Zampieri D, Grazia Mamolo M, Vio L, Banfi E, Scialino G, Fermeglia M, et al. Synthesis, antifungal and antimycobacterial activities of new bis-imidazole derivatives, and prediction of their binding to P45014DM by molecular docking and MM/PBSA method. Bioorganic & Medicinal Chemistry. 2007;15(23):7444-58.
27. Bouchal B, Abrigach F, Takfaoui A, Errahhali ME, Errahhali ME, Dixneuf PH, et al. Identification of novel antifungal agents: antimicrobial evaluation, SAR, ADME–Tox and molecular docking studies of a series of imidazole derivatives. BMC Chemistry. 2019;13(1).
28. Abdelhamid R, Soliman ERS, Mohamed E, Elsaba YM. Epigenetic modulation of Ceratorhiza hydrophila by 5-azacytidine enhances antifungal metabolite production: insights from antimicrobial, metabolic, genomic and computational analyses. BMC Microbiology. 2025;25(1).
29. Babalola BA, Adegboyega AE. Computational Discovery of Potent Imidazole Derivatives as Inhibitors of SARS-CoV-2 Main Protease: An Integrated Approach Combining Molecular Dynamics and Binding Affinity Analysis. Research Square (Research Square). 2023.
30. Danne AB, Deshpande MV, Sangshetti JN, Khedkar VM, Shingate BB. New 1,2,3-Triazole-Appended Bis-pyrazoles: Synthesis, Bioevaluation, and Molecular Docking. ACS Omega. 2021;6(38):24879-90.
31. Anwer KE, Hamza ZK, Ramadan RM. Synthesis, spectroscopic, DFT calculations, biological activity, SAR, and molecular docking studies of novel bioactive pyridine derivatives. Scientific Reports. 2023;13(1).
32. Al-Hazmi GH, Marrakkur V, Naik L, Refat MS. Studies on Photophysical and Biological Activity of Newly Synthesized of 4-Methylpiperidin-4-ol Substituted Pyrazole Derivatives. Polish Journal of Environmental Studies. 2024;33(5):5557-65.
33. Anantacharya R, Satyanarayan ND, Patil S, Mahadevan KM, Adarsha HJ. IN VITRO ANTIOXIDANT, ANTIMICROBIAL AND ADMET STUDY OF NOVEL FURAN/BENZOFURAN C-2 COUPLED QUINOLINE HYBRIDS. International Journal of Pharmacy and Pharmaceutical Sciences. 2017;9(10):144-.
34. Tailor R, Prajapati K, Isa MA, Kappo AP. Synthesis, molecular dynamics simulation and antimicrobial activity of novel s-triazine clubbed with three different hybrid pharmacophores. Biochemical and Biophysical Research Communications. 2025;749:151358-.
35. Sroor FM, El-Sayed AF, Abdelraof M. Investigation of New Biologically Active Benzo[4,5]imidazo[1,2-a]pyrimidine Derivatives as Broad-Spectrum Antimicrobial Agents: Synthesis, Anti-Biofilm, ROS and in Silico Studies. Drug Development Research. 2025;86(3).
36. Aytar EC, Aydın B, Durmaz A, Torunoğlu Eİ. Phytochemical, antioxidant, and antimicrobial properties of Bellardia trixago methanol and ethanol extracts: insights from ADMET and molecular docking approaches. Journal of Food Science and Technology. 2025.